Microchemical Journal 133 (2017) 272–278

Contents lists available at ScienceDirect

Microchemical Journal

journal homepage: www.elsevier.com/locate/microc

Double-pulse laser induced breakdown spectroscopy in orthogonal beam geometry to enhance line emission intensity from agricultural samples

Gustavo Nicolodelli [a], Giorgio S. Senesi [b], Anielle C. Ranulfi [a], Bruno S. Marangoni [c], Alex Watanabe [a], Vinícius de Melo Benites [d], Patrícia P.A. de Oliveira [e], Paulino Villas-Boas [a], Débora M.B.P. Milori [a,*]

[a] Embrapa Instrumentation, P.O. Box 741, 13561-206 São Carlos, SP, Brazil.
[b] CNR, Istituto di Nanotecnologia (NANOTEC) – PLasMI Lab, Bari, 70126 Bari, Italy
[c] Instituto de Física, Universidade Federal do Mato Grosso do Sul, P.O. Box 549, 79070-900 Campo Grande, MS, Brazil
[d] Embrapa Solos, Rua Jardim Botânico 1024, 22460-000 Rio de Janeiro, RJ, Brazil
[e] Embrapa Pecuária Sudeste, P.O. Box 741, 13560-970 São Carlos, SP, Brazil

ARTICLE INFO

Article history:
Received 16 December 2016
Received in revised form 9 March 2017
Accepted 10 March 2017
Available online 30 March 2017

Keywords:
Soil
Plant
Fertilizer
DP LIBS analysis
Orthogonal geometry
Ablative energy

ABSTRACT

A soil, a plant and a fertilizer sample were investigated by double-pulse (DP) laser-induced breakdown spectroscopy (LIBS) in orthogonal beam geometry using a reheating configuration. The DP-LIBS signal enhancement was evaluated with respect to the corresponding single-pulse (SP) LIBS as a function of the interpulse delay at various ablation energies. The maximum signal enhancement measured was 155-fold when low ablation energy (4 mJ) and an interpulse delay of 10 μs were used. At high laser energies (≥16 mJ) and interpulse delay of 0.6 μs, the maximum signal enhancement was up to 3-fold. The effect of excitation energies and interpulse delays on emission line intensities was discussed in the various conditions used. The emission line enhancement measured for ionic lines was always higher than that of atomic lines. Plasma excitation temperature and electron density measured as a function of interpulse delays at various ablation energies were shown to be related to the emission line intensities.

1. Introduction

Over the past decades the use of laser-induced breakdown spectroscopy (LIBS) technique has become an attractive tool for the elemental analysis of agricultural samples of various nature and origin. For example, LIBS has been applied successfully as an alternative method to quantify toxic elements, macro and micronutrients and C in soils [1–3], and macronutrients such as N, K and P and other relevant elements, including Al, Ca, Mg and Si, in fertilizers [4–9]. Further, LIBS was shown to be a fast, suitable and reliable technique for the simultaneous qualitative and quantitative analysis of macro and micronutrients in different plant leaves, and even in disease diagnoses [10–14].

In recent years, the need to increase and optimize LIBS analytical performances, e.g. by decreasing the limit of detection (LOD) of some elements and the signal enhancement of emission lines, has become an urgent issue in various applications. In general, a feasible signal enhancement can be achieved by a high number of accumulated shots [15] or fluence delivered to the sample [13,16], but this is often not fair when analyzing samples of limited amount available, especially in the case of biological, environmental and cultural heritage materials. In the single pulse (SP) LIBS, the signal improvement can be obtained by the proper choice of operational parameters, including excitation wavelength, pulse duration, repetition rate, pulse energy, number of accumulated pulses, surrounding atmosphere, laser focusing and collecting optics, and/or spectrometer parameters such as delay time and integration time gate [13,15–17]. However, a signal improvement can also be obtained by improving the conventional LIBS system, e.g. using a resonant excitation system [18] or double pulse (DP) LIBS [17,19–32].

In particular, the DP LIBS system uses a second laser pulse after the typical single pulse, thus enhancing line emission intensities and improving the signal-to-noise ratio. The DP LIBS can be operated in different configurations, i.e. collinear, crossed beam or orthogonal, which allows preablation and reheating. In the DP LIBS orthogonal configuration the signal intensity can be increased by increasing the laser energy and/or the number of pulses without increasing the amount of ablated material [21,22,24,26,29,30]. The preservation of the physical structure of samples is particularly useful when analyzing samples in the form of soft and brittle pellets and for cultural heritage artifacts. However, in the DP orthogonal configuration a high signal-to-noise ratio can be retained even at relatively low power density [26,29].

* Corresponding author at: Embrapa Instrumentation, Rua XV de Novembro, 1452, Centro, P.O. Box 741, 13561-206, Sao Carlos, SP, Brazil.
E-mail address: debora.milori@embrapa.br (D.M.B.P. Milori).

http://dx.doi.org/10.1016/j.microc.2017.03.047
0026-265X/

As far as we know all previous studies using DP LIBS in orthogonal geometry in the reheating mode have been performed on metals and metallic alloys [21,22,24,26,29,30]. Differently, this study was focused on chemically-complex matrices such as agricultural samples containing high amounts of organic matter (e.g. plants) or a prevalent inorganic composition (e.g. soils and fertilizers). Sample matrix composition is indeed crucial in laser/matter interactions and subsequent laser induced plasma formation and emission.

The detection of micronutrients and toxic elements present in agricultural samples is generally limited when using conventional SP LIBS mode due to the low concentration of these elements. Thus, the main aim of this study was to explore the potential of DP LIBS using a reheating scheme in the orthogonal beam geometry to improve LIBS analytical performance with respect to SP LIBS. In particular, this study aimed to investigate the effect of different laser ablation energies and interpulse delays on emission line intensities, also evaluating the effects of plasma excitation temperature and electron density. A further aim was to establish a correlation between the atomic states, excitation energy levels and intensity increases for a number of different emission lines. To achieve these purposes, an echelle spectrometer was used, which was able to collect many emission lines simultaneously on a large spectral window as a function of the excitation energy levels, which is not possible by a monochromator.

2. Materials and methods

2.1. Samples

The soil sample was a Red Latosol collected at a depth of 100 cm under a Brazilian forest (Atlantic Forest) in an area of the Southeast Livestock Research Center of Embrapa located in São Carlos, São Paulo State, Brazil. The fertilizer sample was an organic mineral fertilizer consisting of a mixture of poultry litter and sugarcane bagasse composted for about 120 days in static piles and then added with phosphate rock at 1:1 ratio (wt%). This sample was selected from the laboratory-prepared Embrapa collection of fertilizers that simulate typical commercial products. To ensure homogeneity, soil and fertilizer samples were dried, sieved to remove roots, and ground to obtain particles smaller than 0.15 mm. The pellets obtained have a diameter of 1.2 mm.

The plant leaves were collected in the field from 5 healthy soybean plants (variety BRS 7589) at the end of the growing season at the Canada farm located in São Carlos, São Paulo State, Brazil. The leaves were first cleaned superficially with distilled water and then oven-dried at 60 °C for 72 h. The homogenized powders obtained after cryogenical milling were pelletized by pressing at 8 tons for 30 s.

2.2. LIBS experiment

The DP experiments were conducted using two laser sources: (a) a Nd:YAG Q-switched Brilliant (Quantel) operating at the wavelength of 532 nm (visible, VIS) and a pulse width of 4 ns used as the ablation laser (laser 1); and (b) a Nd:YAG Q-switched Ultra (Quantel) laser operating at the wavelength of 1064 nm (near-infrared, NIR) and a pulse width of 6 ns used as the reheating laser (laser 2) to reexcite ablated atoms and ions. Lasers producing shorter wavelength radiation are known to be more effective for material ablation due to their capacity of reducing plasma shielding, whereas lasers producing NIR radiation are more effective for reheating the plasma [33,34]. The plasma initiation with nanosecond lasers is provoked by two processes; the first one is inverse Bremsstrahlung by which free electrons gain energy from the laser during collisions among atoms and ions. The second one is photoionization of excited species and excitation of ground atoms with high energies [35]. Laser coupling is better with shorter wavelengths, but at the same time the threshold for plasma formation is higher. This is because inverse Bremsstrahlung is more favorable for NIR wavelengths [36]. Thus, to increase LIBS performances the DP process consists of two distinct steps, i.e. ablation and excitation, each performed at the most appropriate laser wavelength.

The pulse from laser 1 was focused by a 10-cm plano-convex lens perpendicular to the target surface employing output energies ranging from 1 to 32 mJ (power density, 40–1280 GW/cm^2). Laser 2 with a peak energy of 50 mJ was focused parallel to the target surface by a 10-cm plano-convex lens, and the focal point was located at ~0.5 mm from the surface. The shot-to-shot stability was monitored by an energy meter (Coherent). Both laser focal points were aligned within a plane normal (x-y axis) to the surface so that the focal point of plasma induced in air by laser 2 was coincident with the perpendicular line from the focal point of laser 1 along the z-axis (orthogonal symmetry). Two silica lenses were placed between the sample and the tip of the fiber to obtain the best optical coupling and the most efficient collection of plasma emission.

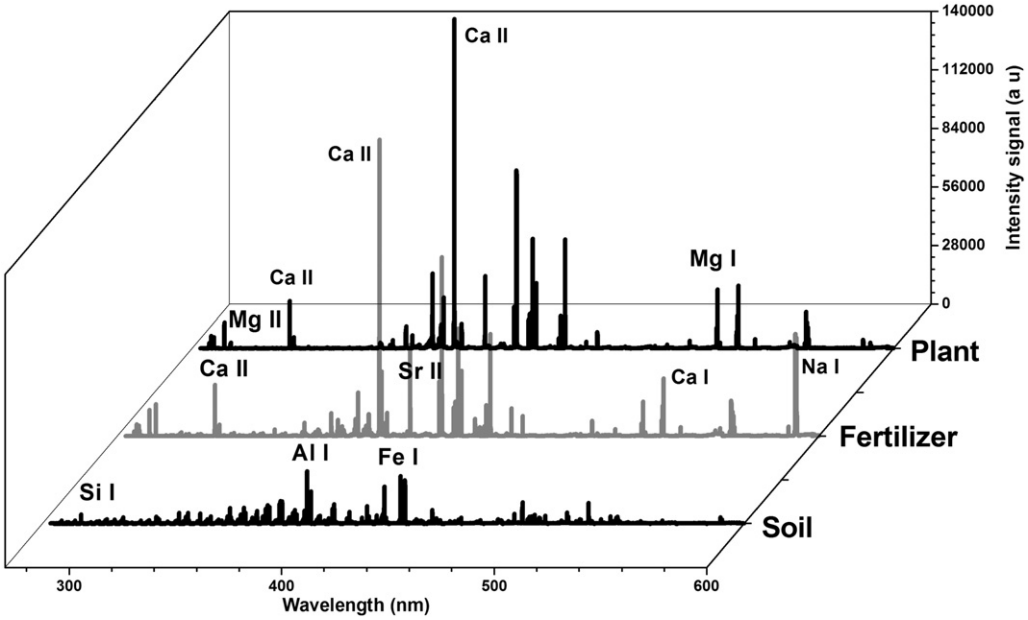

Fig. 1. DP LIBS spectra in the VIS range of the soil, plant and fertilizer samples examined.

The spectrometer echelle (Aryelle Butterfly 400) operated in two spectral bands, i.e. 175–330 nm and 275–750 nm, with a spectral resolution of 13–24 pm and 29–80 pm, respectively. The detector used was an intensified charge-coupled device (ICCD) camera with 1024 × 1024 pixels. The effect of the interpulse delay was investigated by performing ten measurements on different locations of the sample surface for each value used. Each measurement was obtained from ten accumulated pulses at a delay time fixed at 1 μs. The sample support was placed in a micro-controlled xy stage for an easy and fast scanning of the laser beam impinging on it.

The SP LIBS spectra were acquired by the same VIS laser beam at the wavelength of 532 nm used in the DP experiments (laser 1) at the same ablation energy. The temporal parameters used in the SP LIBS setup were optimized to obtain the best signal-to-noise ratio using a delay time at 1 μs.

The SP LIBS and DP LIBS spectra were studied by comparing 10 SP LIBS spectra for each output energy and 10 DP LIBS spectra obtained for each parameter tested, i.e. output energies of 1, 4, 8, 16 and 32 mJ and interpulse delays of 0.2, 0.6, 1, 3, 5, and 10 μs. Results were analyzed systematically as the ratios between the intensity area of the line obtained in DP experiments and that obtained in SP experiments. The intensity corresponded to the difference between the signal and the background that was evaluated and corrected by subtracting the average noise region near each element emission line. Each intensity area was calculated by Lorentzian fitting of one peak emission in each spectrum, and then averaging the ten areas obtained.

3. Results and discussion

As an example, Fig. 1 shows the LIBS spectra in the VIS range in orthogonal DP configuration of the soil, fertilizer and plant samples obtained using an interpulse delay of 3 μs, a delay time of 1 μs and an ablation energy of 4 mJ. The interpulse delay between the LIBS plume

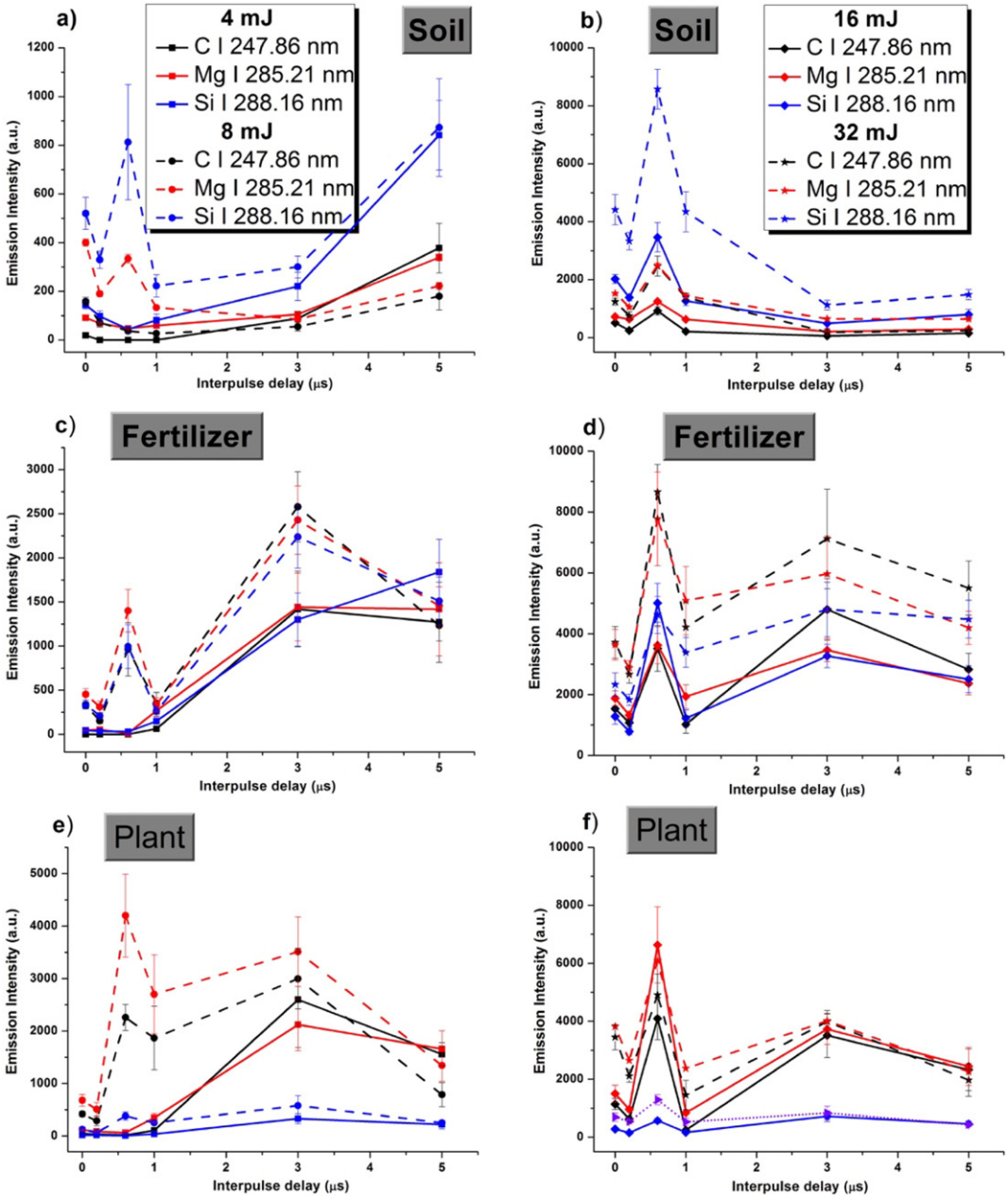

Fig. 2. Emission intensities of atomic lines of C at 247.86 nm, Mg at 285.21 nm and Si at 288.16 nm measured for the soil (a–b), fertilizer (c–d) and plant (e–f) samples as a function of interpulse delays (0.2, 0.6, 1, 3, 5 μs) at different ablation energies (4, 8, 16, 32 mJ).

generation laser and the reheating laser is one of the main parameters that affects the signal enhancement in DP LIBS.

Fig. 2 a to f show the trends of LIBS atomic emission intensities of the C line at 247.86 nm, the Mg line at 285.21 nm and the Si line at 288.16 nm measured for the soil, fertilizer and plant samples as a function of different interpulse delays (from 0 to 5 μs) at four different ablation energies (4, 8, 16 and 32 mJ). Data show that the signal enhancement is strongly dependent on the interpulse delay and ablation energy values used throughout plasma expansion. In particular, at higher ablation energies (16 and 32 mJ) the optimal interpulse delay value is 0.6 μs for all samples, whereas at lower ablation energies (4 and 8 mJ) this value varies as a function of the sample examined. In particular, the higher emission intensity enhancement for the soil sample is generally at 5 μs, whereas for plant and fertilizer samples is generally at 3 μs. An interpulse value of zero corresponds to measurements obtained by the optimized SP LIBS system. The LIBS spectra in the SP and DP modes measured by applying an ablation energy of 1 mJ at interpulse delays < 1 μs show no emission lines. Further, the existing plasma cannot reabsorb the energy of the second laser beam at high interpulse delays, i.e. 10 μs, because it results too expanded and the electronic density too low, thus no signal increase can be achieved.

A possible explanation of the optimal interpulse delay obtained at low pulse energy (Fig. 2 a, c, e) was provided by Sangines et al. [26] on the basis of the shockwave and plume dynamics of plasma expanding in a gas environment. In particular, when the interpulse delay grows the signal enhancement decreases as the second pulse finds a reduced density plume due to its expansion through the background atmosphere. However, in the μs timescale a steeper signal enhancement occurs reaching the optimal value at low energy [26]. Tognoni et al. [17] found that at interpulse values lower than 100 μs, the ablation plume presents the largest particle density, which increases the absorption of the second pulse. Further, low ablation energies appear enough to vaporize the material and produce a less dense plasma, but not enough to be absorbed by the plasma due to the plasma shielding process, i.e. a weak or null absorption of the trailing part of the ablation pulse occurs, which may lead to a weak plume emission [17,26,35]. Thus, when the second pulse hits the vaporized material, the absorption process via inverse Bremsstrahlung may become significant thus contributing to a larger signal enhancement [26,37].

Fig. 3 shows the intensity enhancement measured for the emission lines of atomic Fe I at 303.74 nm and ionic Fe II 238.81 nm in the soil sample, atomic Ca I at 527.03 nm and ionic Ca II at 315.89 nm in the fertilizer sample, and atomic Mg I 285.21 and ionic Mg II 280.27 in the plant sample, as a function of interpulse delays at 16 and 32 mJ ablation energies. In particular, at higher ablation energies (16 and 32 mJ) the optimal interpulse delay value is confirmed to be 0.6 μs. Data show a substantial signal enhancement of ionic lines originated from high excitation energy levels, with respect to atomic lines.

The greater is the energy of the reheating pulse, the more important is the energy absorbed by the plasma, which induces a higher population in the upper states with high excitation energies. This result can be explained by the fact that all energy of the reheating laser is spent to increase plasma temperature and to excite ions, which leads to the enhancement of the emission intensity from ions, while the emission from atoms remains the same, or even decreases, due to additional ionization. Similar results were obtained by Gautier et al. [22] and Oba et al. [38] on samples of different nature. As the reheating pulse directed in the plasma does not ablate further matter, the observed enhancements would not be due to an increased ablation.

At high energies, the maximum intensity is obtained at 32 mJ and interpulse delay of 0.6 μs for all samples (Fig. 2 b, d, f, and Fig. 3). This result is in agreement with findings of Gautier et al. [21] who obtained the best results for low interpulse delay (0.2 μs) by using high energies. When the power density increases, also the plume density increases, which changes the features of plasma expansion, i.e. the ablation pulse possesses enough energy to vaporize the material producing a highly dense plasma that favors plasma shielding processes. Due to changed plasma features the best interpulse delay value also changes, i.e. at values lower than 1 μs the shock waves formed by the first pulse shield the interaction with the second pulse, thus avoiding its coupling

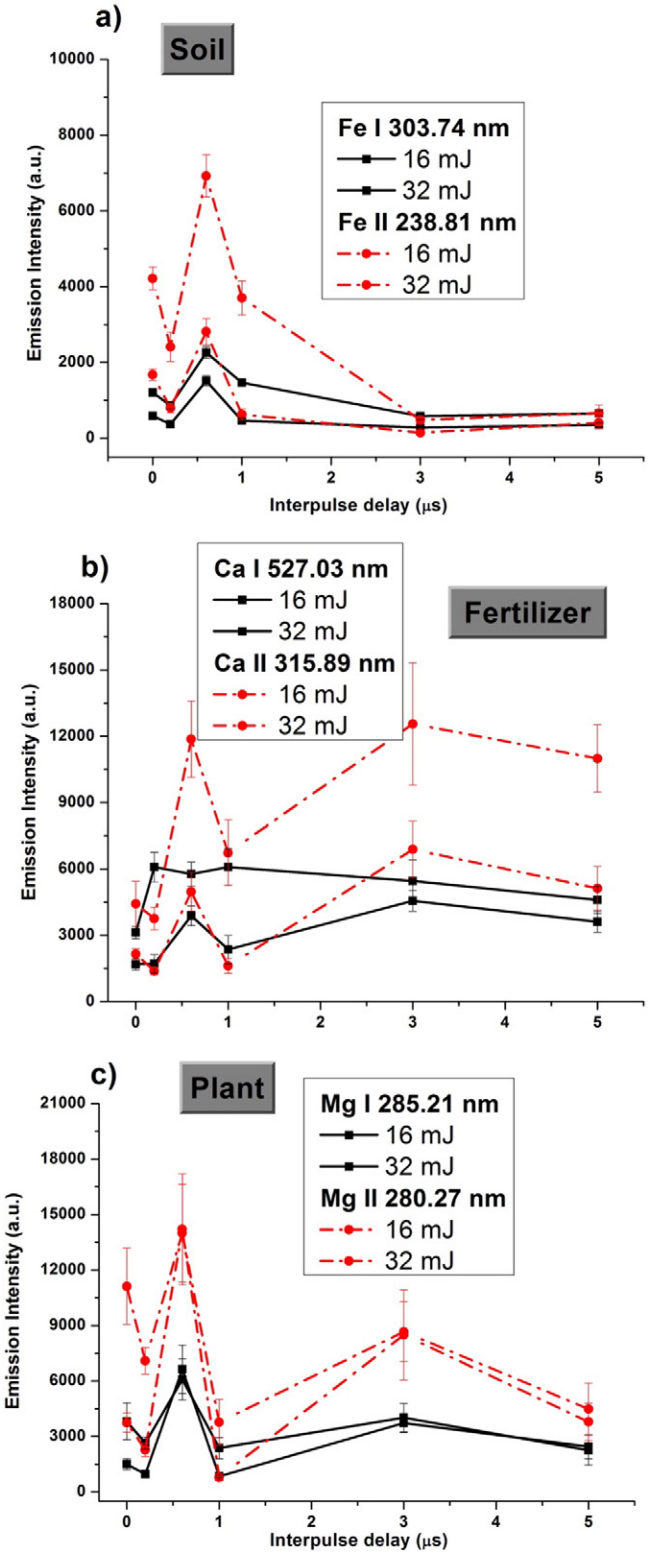

Fig. 3. Emission intensities of atomic and ionic lines of Fe I at 303.74 nm and Fe II at 238.81 nm (a), Ca I at 527.03 nm and Ca II at 315.89 nm (b) and Mg I at 285.21 nm and Mg II at 280.27 nm (c) measured, respectively, for the soil, fertilizer and plant samples as a function of interpulse delays (0.2, 0.6, 1, 3, 5 μs) at higher ablation energies (16 and 32 mJ).

Table 1
Optimal parameters for obtaining the highest intensity enhancement of emission lines in the reheating DP LIBS experiments.

Samples	Element	Emission line wavelength (nm)	Parameters		DP/SP line intensity Ratio	Upper energy level (eV)	RSD of Emission Intensities		*P* value
			Interpulse delay (us)	Energy laser 1 (mJ)			SP	DP	
Soil	Fe II	238.810	10	4	71	7.77	13.5	12.9	$0.84\ 10^{-5}$
	Fe II	241.027	10	4	61	10.38	19.0	7.2	$0.01\ 10^{-5}$
	C I	247.856	10	4	61	7.68	17.5	11.0	0.02
	Fe II	258.588	10	4	53	4.79	21.1	17.6	0.03
	Fe II	273.955	10	4	53	5.51	21.0	11.2	$2.3\ 10^{-5}$
	Mg II	280.270	10	4	34	4.42	26.5	13.7	$7.1\ 10^{-6}$
	Mg I	285.213	5	4	11	4.35	10.3	8.5	$2.2\ 10^{-3}$
	Si I	288.158	10	4	19	5.08	11.3	13.5	$9.9\ 10^{-7}$
	Fe I	303.738	10	4	15	4.19	17.6	7.9	$3.4\ 10^{-8}$
	Ti II	307.864	10	4	21	4.05	11.8	23.9	$7.4\ 10^{-5}$
Fertilizer	C I	247.856	3	8	8	7.68	8.8	15.0	$5.0\ 10^{-5}$
	P I	255.326	3	8	10	7.17	27.3	10.7	$3.9\ 10^{-5}$
	Mg II	280.270	10	4	155	4.42	21.0	12.5	$1.8\ 10^{-6}$
	Mg I	285.213	10	4	49	4.35	8.7	13.2	$1.6\ 10^{-4}$
	Si I	288.158	10	4	45	5.08	18.0	21.3	$2.1\ 10^{-4}$
	Ca II	315.887	3	8	10	7.04	13.9	16.7	$1.2\ 10^{-5}$
	Ca II	393.366	10	4	37	3.15	9.4	25	0.04
	Sr II	407.77	5	4	32	3.04	18.8	14.8	$2.8\ 10^{-5}$
	Sr I	460.733	3	4	8	2.69	6.6	14.0	$3.9\ 10^{-4}$
	Ca I	527.027	3	4	10	4.87	17.0	16.0	$5.8\ 10^{-4}$
	Fe I	714.815	3	4	10	7.09	13	15	$9.3\ 10^{-4}$
Plant	C I	247.856	3	4	57	7.68	14	35	$2.2\ 10^{-3}$
	Mg II	280.27	1	8	7	4.42	16	29	$1{,}6\ 10^{-2}$
	Mg I	285.213	3	4	19	4.35	23	16	$3.5\ 10^{-6}$
	Si I	288.158	3	4	18	5.08	36	28	$3.4\ 10^{-3}$
	Ca II	315.887	3	4	33	7.04	28	19	$8.9\ 10^{-6}$
	Ca II	393.366	3	4	23	3.15	24	16	$1.3\ 10^{-5}$

in the plasma, with a consequent reheating effect and signal enhancement. Differently, at interpulse delays higher than 1 μs, the ablation effect of the first pulse becomes dominant when a high ablation energy is used, thus leading to limited improvement of DP LIBS signals (up to 3 times) with respect to SP LIBS ones. All thermal processes, including plasma heating, are less important in this case, i.e. the plasma is already

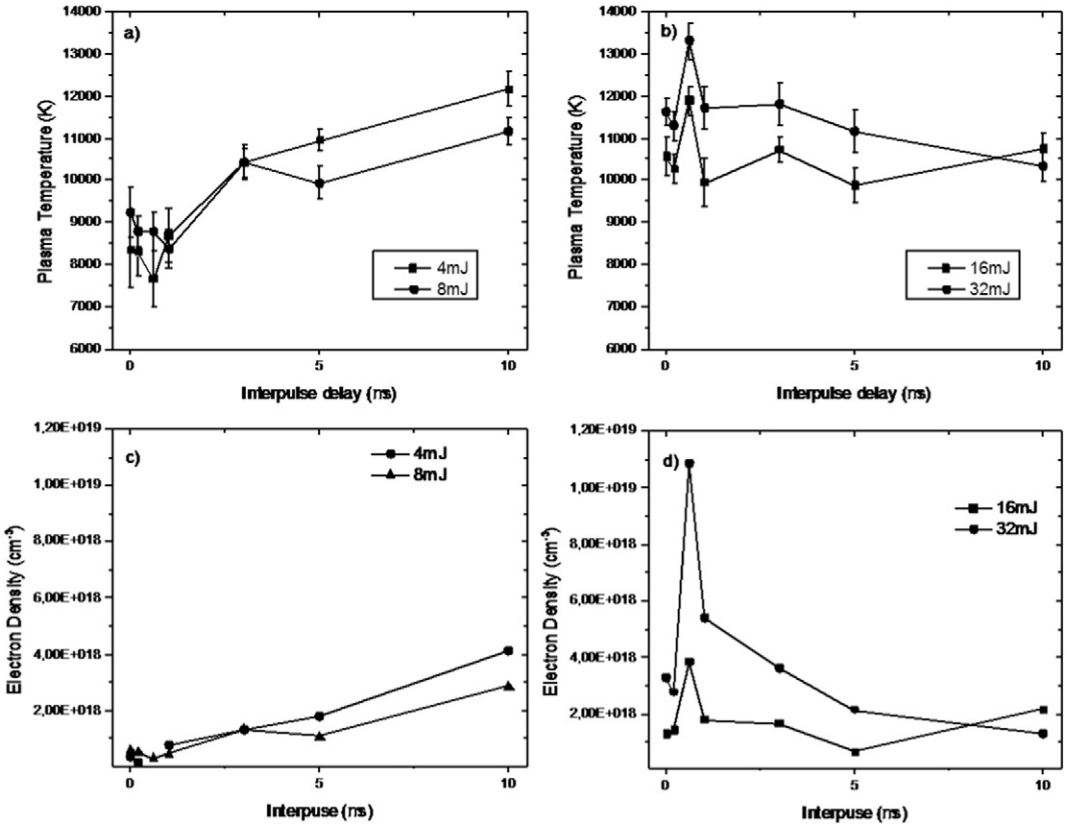

Fig. 4. Plasma temperature (a–b) and electron density (c–d) as a function of interpulse delays (0.2, 0.6, 1, 3, 5, 10 μs) at low (left) and high (right) ablation energies for the fertilizer sample.

close to its optimal state due to the emission reabsorption by plasma shielding effect.

The extent of the shielding effect depends not only on the experimental variables used (buffer gas composition and pressure, laser wavelength and irradiance), but also on the sample nature [17]. For metal samples, the ablated mass is strongly affected by the ambient pressure, but for agricultural samples this effect is relatively small, which confirms the relevant influence of sample characteristics at the beginning of the plasma generation processes. Different behaviors are also expected as a function of the thermal diffusivity of the sample, which determines the speed of heat diffusion from the target surface to the bulk and, in turn, the spatial distribution of the temperature inside the target and the depth of the crater.

In order to evaluate the increase of emission line intensities measured in the DP mode with respect to the SP mode, the ratios of intensities in the DP and SP mode were calculated for some relevant lines measured in the three samples. For all samples the highest intensity enhancement of all emission lines was measured at low excitation energies, in most cases 4 mJ, and interpulse delays varying between 3 and 10 μs (Table 1). These results well agree with those obtained for metal alloys by Contreras et al. [29] and Sanginês et al. [26]. The similar behavior shown by different emission lines and different samples confirms the robustness of results obtained. The intensity signal ratio DP/SP could not be calculated at low ablation energy (1 mJ), because the emission peak intensity in the SP mode at this energy was below the LOD of the technique. According to Tognoni et al. [17], plasma reheating allows to obtain detectable signals when using very low energy ablation pulses or after long delays from plasma ignition, which yields a complete atomization of ablated particles. The results obtained in this optimization study conducted at low excitation energies are relevant especially for samples that require a small damage, such as cultural heritage samples, where intense ablative thermal processes should be avoided.

The relative standard deviation (RSD) of the intensity of different emission lines was calculated for SP and DP LIBS mode, the values are shown in Table 1. Mainly the DP LIBS data are more accurate and report the most of the emission lines with a smaller RSD value compared to the SP LIBS data. Further, the Shapiro-Wilk normality test was applied to verify the hypotheses on SP and DP emission intensity data. The data obtained were significant and from a normally distributed population. The Paired Sample *t*-test was also applied, at the 0.05 level, finding different population and so significant variation from the test difference.

The excitation temperature and electron density were also measured as a function of the interpulse delay at both low and high excitation energies for the fertilizer sample (Fig. 4). The electron excitation temperature was determined by applying the Boltzmann plot method to the Ca emission lines at 430.25 nm, 430.77 nm, 445.48, 445.59, 612.22 nm and 616.22 nm. The electron density was calculated using the Saha-Boltzmann equation [39] from the ratios between atomic and ionic line intensities of Ca at 612.22 nm and 370.60 nm, respectively for low and high ablation energies. Both trends are similar to the trends measured for emission line intensities (C I, Mg I and Si I) shown in Fig. 2. In particular, the highest temperature and electron density were reached at an interpulse delay of 0.6 μs when using high energies (16 and 32 mJ), and at an interpulse delay of 10 μs at low energies (4 or 8 mJ). These results confirm that the enhancement of LIBS emission line intensities is clearly associated to the increased plasma temperature and electron density.

4. Conclusions

The optimization of orthogonal DP LIBS configuration through the optimization of excitation energy and interpulse delay values allowed to enhance LIBS analytical performance for agricultural samples including soil, fertilizer and plant in terms of signal-to-noise ratio increase, signal intensity enhancement and sample damage minimization. Although a relatively high signal-to-noise ratio could still be retained, the emission line intensities measured at lower excitation energies using the orthogonal DP configuration were up to 155 times higher than those obtained by SP LIBS.

Further, the absolute novelty of this work consists in the study of the best interpulse delay value to be used at various ablation energies in order to obtain the highest line emission intensity from the samples examined. However, the signal enhancement depends on several experimental parameters, and the enhancement factor induced by the reheating approach depends on the type of line emissions, i.e. atomic or ionic lines. In the present experiments, the maximum enhancement was measured for ionic lines.

The use of low ablative energies and the production of high signal emissions are fundamental issues in LIBS, especially when dealing with agricultural samples. This because the sample pellets used can be easily damaged or destroyed when high ablative energies and long accumulation shots are applied on the same spot. Further, the robustness of results obtained is confirmed by the good correspondence between the trends of plasma temperature and electron density and that of emission line intensities at the various interpulse delays tested for the samples studied.

The signal enhancement in the DP LIBS can be due to several mechanisms, and the relative importance of each is still subject to discussion. However, results of this study, besides providing a contribution to the current evaluation of the DP approach, can also contribute to better understanding the influence of laser wavelength on laser–target and laser-plasma interactions.

Acknowledgments

The authors thank FAPESP (Process: 2012/24349-0 and 2013/07276-1) and CNPq (grant number 461743/2014-0) for their financial support of this study.

References

[1] E.C. Ferreira, D.M.B.P. Milori, E.J. Ferreira, L.M. Dos Santos, L. Martin-Neto, A.R. de A. Nogueira, Evaluation of laser induced breakdown spectroscopy for multielemental determination in soils under sewage sludge application, Talanta 85 (1) (2006) 435–440, http://dx.doi.org/10.1016/j.talanta.2011.04.001.

[2] G.S. Senesi, M. Dell'Aglio, R. Gaudiuso, A. De Giacomo, C. Zaccone, O. De Pascale, T.M. Miano, M. Capitelli, Heavy metal concentrations in soils as determined by laser-induced breakdown spectroscopy (LIBS), with special emphasis on chromium, Environ. Res. 109 (4) (2009) 413–420, http://dx.doi.org/10.1016/j.envres.2009.02.005.

[3] G. Nicolodelli, B.S. Marangoni, J.S. Cabral, P.R. Villas Boas, G.S. Senesi, C.H. Santos, R.A. Romano, A. Segnini, Y. Lucas, C.R. Montes, D.M.B.P. Milori, Quantification of total carbon in soil using laser-induced breakdown spectroscopy: a method to correct interference lines, Appl. Opt. 53 (10) (2014) 2170–2176, http://dx.doi.org/10.1364/AO.53.002170.

[4] M. Ga, I. Sapir-Sofer, H. Modiano, R. Stana, Laser induced breakdown spectroscopy for bulk minerals online analyses, Spectrochim, Acta Part B 62 (12) (2007) 1496–1503, http://dx.doi.org/10.1016/j.sab.2007.10.041.

[5] M. Ga, Y. Groisman, Online analysis of potassium fertilizers by laser-induced breakdown spectroscopy, Spectrochim, Acta Part B 65 (8) (2010) 744–749, http://dx.doi.org/10.1016/j.sab.2010.03.019.

[6] B.S. Marangoni, K.S.G. Silva, G. Nicolodelli, G.S. Senesi, J.S. Cabral, P.R. Villas-Boas, C.S. Silva, P.C. Teixeira, A.R. A. Nogueira, V.M. Benites, D.M.B.P. Milori, Phosphorus quantification in fertilizers using laser induced breakdown spectroscopy (LIBS): a methodology of analysis to correct physical matrix effects, Anal. Methods. 8 (2016) 78–82, http://dx.doi.org/10.1039/C5AY01615K.

[7] D.F. Andrade, E.R. Pereira Filho, Direct determination of contaminants, major and minor nutrients in solid fertilizers using laser-induced breakdown spectroscopy (LIBS), J. Agric. Food Chem. 64 (2016) 7890–7898.

[8] W.A. Farooq, F.N. Al-Mutairi, A.E.M. Khater, A.S. Al-Dwayyan, M.S. AlSalhi, M. Atif, Elemental analysis of fertilizer using LaserInduced breakdown spectroscopy opt, Spectroscopy 112 (2012) 874–880.

[9] L.C. Nunes, A. Carvalho, G. Gustinellil, D.S. Junior, F.J. Krug, Determination of Cd, Cr and Pb in phosphate fertilizers by laser-induced breakdown spectroscopy, Spectrochim. Acta A 97 (2014) 42–48.

[10] G.S. Senesi, M. DellAglio, A. De Giacomo, O. De Pascale, Z. Al Chami, T.M. Miano, C. Zaccone, Elemental composition analysis of plants and composts used for soil remediation by laser-induced breakdown spectroscopy, clean – soil, air, Water 42 (2014) 791–798, http://dx.doi.org/10.1002/clen.201300411.

[11] D. Santos Jr., L.C. Nunes, G.G.A. Carvalho, M.S. Gomes, P.F. Souza, F.O. Leme, L.G.C. Santos, F.J. Krug, Laser-induced breakdown spectroscopy for analysis of plant materials: a review, Spectrochim. Acta, Part B 71 (2012) 3–13.

[12] L.C. Nunes, J.W.B. Braga, L.C. Trevizan, P.F. Souza, G.G.A. Carvalho, D. Santos Jr., R.J. Poppi, F.J. Krug, Optimization and validation of a LIBS method for the determination of macro and micronutrients in sugar cane leaves, J. Anal. At. Spectrom. 25 (2010) 1453–1460, http://dx.doi.org/10.1039/C003620J.
[13] G.G.A. de Carvalho, D.S. Junior, L.C. Nunes, M. da Silva Gomes, F. de O. Leme, F.J. Krug, Effects of laser focusing and fluence on the analysis of pellets of plant materials by laser-induced breakdown spectroscopy, Spectrochim. Acta B 74–75 (2012) 162–168, http://dx.doi.org/10.1016/j.sab.2012.06.012.
[14] F.M.V. Pereira, D.M.B.P. Milori, A.L. Venâncio, M. de S. T. Russo, P.K. Martins, J. Freitas-Astúa, Evaluation of the effects of Candidatus Liberibacter asiaticus on inoculated citrus plants using laser-induced breakdown spectroscopy (LIBS) and chemometrics tools, Talanta 83 (2010) 351–356, http://dx.doi.org/10.1016/j.talanta.2010.09.021.
[15] D.W. Hahn, N. Omenetto, Laser-induced breakdown spectroscopy (LIBS), part II: review of instrumental and methodological approaches to material analysis and applications to different fields, Appl. Spectrosc. 66 (4) (2012) 347–419, http://dx.doi.org/10.1366/11-06574.
[16] J.-B. Sirven, P. Mauchien, B. Sallé, Analytical optimization of some parameters of a laser-induced breakdown spectroscopy experiment, Spectrochim. Acta B At. Spectrosc. 63 (2008) 1077–1084, http://dx.doi.org/10.1016/j.sab.2008.08.013.
[17] E. Tognoni, G. Cristoforetti, Basic mechanisms of signal enhancement in ns double-pulse laser-induced breakdown spectroscopy in a gas environment, J. Anal. At. Spectrom. 29 (2014) 1318–1338, http://dx.doi.org/10.1039/C4JA00033A.
[18] H. Kondo, N. Hamada, K. Wagatsuma, Determination of phosphorus in steel by the combined technique of laser induced breakdown spectrometry with laser induced fluorescence spectrometry, Spectrochim. Acta, Part B 64 (2009) 884–890.
[19] J. Uebbing, J. Brust, W. Sdorra, F. Leis, K. Niemax, Reheating of a laser-produced plasma by a second pulse laser, Appl. Spectrosc. 45 (9) (1991) 1419–1423.
[20] L. St-Onge, V. Detalle, M. Sabsabi, Enhanced laser-induced breakdown spectroscopy using the combination of fourth-harmonic and fundamental Nd:YAG laser pulses, Spectrochim. Acta Part B 57 (1) (2002) 121–135, http://dx.doi.org/10.1016/S0584–8547(01)00358-5.
[21] C. Gautier, P. Fichet, D. Menut, J.L. Lacour, D. L'Hermite, J. Dubessy, Study of the double-pulse setup with an orthogonal beam geometry for laser-induced breakdown spectroscopy, Spectrochim. Acta Part B 59 (7) (2004) 975–986.
[22] C. Gautier, P. Fichet, D. Menut, J.-L. Lacour, D. L'Hermite, J. Dubessy, Quantification of the intensity enhancements for the double-pulse laser-induced breakdown spectroscopy in the orthogonal beam geometry, Spectrochim. Acta Part B 60 (2) (2005) 265–276.
[23] M. Corsi, G. Cristoforetti, M. Hidalgo, S. Legnaioli, V. Palleschi, A. Salvetti, E. Tognoni, C. Vallebona, Double pulse, calibration-free laser-induced breakdown spectroscopy: a new technique for in situ standard-less analysis of polluted soils, Appl. Geochem. 21 (5) (2006) 748–755.
[24] G. Cristoforetti, Orthogonal double-pulse versus single-pulse laser ablation at different air pressures: a comparison of the mass removal mechanisms, Spectrochim. Acta Part B 64 (1) (2009) 26–34.
[25] G. Nicolodelli, G.S. Senesi, R.A. Romano, I.L.O. Perazzoli, D.M.B.P. Milori, Signal enhancement in collinear double-pulse laser-induced breakdown spectroscopy applied to different soils, Spectrochim. Acta Part B 111 (2015) 23–29.
[26] R. Sanginés, V. Contreras, H. Sobral, A. Robledo-Martinez, Optimal emission enhancement in orthogonal double-pulse laser-induced breakdown spectroscopy, Spectrochim. Acta Part B 110 (2015) 139–145, http://dx.doi.org/10.1016/j.sab.2015.06.012.
[27] V. Piscitelli, M.A. Martínez, A.J. Fernández, J.J. González, X.L. Mao, R.E. Russo, Double pulse laser induced breakdown spectroscopy: experimental study of lead emission intensity dependence on the wavelengths and sample matrix, Spectrochim. Acta Part B 64 (2) (2009) 147–154, http://dx.doi.org/10.1016/j.sab.2008.11.008.
[28] G. Nicolodelli, G.S. Senesi, I.L.O. Perazzoli, B.S. Marangoni, V.M. Benites, D.M.B.P. Milori, Double pulse laser induced breakdown spectroscopy: a potential tool for the analysis of contaminants and macro/micronutrients in organic mineral fertilizers, Sci. Total Environ. 565 (2016) 1116–1123, http://dx.doi.org/10.1016/j.scitotenv.2016.05.153.
[29] V. Contreras, M.A. Meneses-Nava, O. Barbosa-García, J.L. Maldonado, G. Ramos-Ortiz, Double-pulse and calibration-free laser-induced breakdown spectroscopy at low-ablative energies, Opt. Lett. 37 (22) (2012) 4591–4593, http://dx.doi.org/10.1364/OL.37.004591.
[30] R. Ahmed, M.A. Baig, A comparative study of enhanced emission in double pulse laser induced breakdown spectroscopy, Opt. Laser Technol. 65 (2015) 113–118.
[31] V.I. Babushok, F.C. DeLucia Jr., J.L. Gottfried, C.A. Munson, A.W. Miziolek, Double pulse laser ablation and plasma: laser induced breakdown spectroscopy signal enhancement, Spectrochim. Acta Part B 61 (9) (2006) 999–1014, http://dx.doi.org/10.1016/j.sab.2006.09.003.
[32] R.W. Coons, S.S. Harilal, S.M. Hassan, A. Hassanein, The importance of longer wavelength reheating in dual-pulselaser-induced breakdown spectroscopy, Appl. Phys. B Lasers Opt. 107 (2012) 873–880.
[33] W. Sdorra, J. Brust, K. Niemax, Basic investigations for laser microanalysis: IV. The dependence on the laser wavelength in laser ablation, Mikrochim. Acta 108 (1992) 1–10.
[34] C. Geertsen, A. Briand, F. Chartier, J.-L. Lacour, P. Mauchien, J.-M. Mermet, S. Sjöström, Comparison between IR and UV laser ablation at atmospheric pressure: implications for solid-sampling ICP-spectrometry, J. Anal. At. Spectrom. 9 (1994) 17–22.
[35] F. Anabitarte, A. Cobo, J.M. Lopez-Higuera, Laser-induced breakdown spectroscopy: fundamentals, applications, and challenges, ISRN Spectroscopy 2012 (2012) 1–12, http://dx.doi.org/10.5402/2012/285240.
[36] L.M. Cabalin, J.J. Laserna, Experimental determination of laser induced breakdown thresholds of metals under nanosecond Q-switched laser operation, Spectrochim. Acta B 53 (1998) 723–730.
[37] X. Mao, R.E. Russo, Observation of plasma shielding by measuring transmitted and reflected laser pulse temporal profiles, Appl. Phys. A Mater. Sci. Process. 64 (1) (1997) 1–6, http://dx.doi.org/10.1007/s003390050437.
[38] M. Oba, Y. Maruyama, K. Akaoka, M. Miyabe, I. Wakaida, Double-pulse LIBS of gadolinium oxideablated by femto- and nano-second laser pulses, Appl. Phys. A Mater. Sci. Process. 101 (2010) 545–549.
[39] M. Corsi, G. Cristoforetti, M. Hidalgo, D. Iriarte, S. Legnaioli, V. Palleschi, A. Salvetti, E. Tognoni, Effect of laser-induced crater depth in laser-induced breakdown spectroscopy emission features, Appl. Spectrosc. 59 (7) (2005) 853–860.